Appendix A

Results for the planar example

This appendix chapter contains the computation results of the planar example from Section 6.1. The example's task is to compute minimum-time trajectories for a planar three-link manipulator along the straight line paths illustrated in Figure A.1 starting from its depicted initial pose

$$q_1\,(t=0) = \frac{1}{6}\pi, \quad q_2\,(t=0) = -\frac{2}{3}\pi, \quad q_3\,(t=0) = \frac{2}{3}\pi.$$

The only physical constraints are joint torque limits of $M_{i,\max} = \pm 10$ Nm.

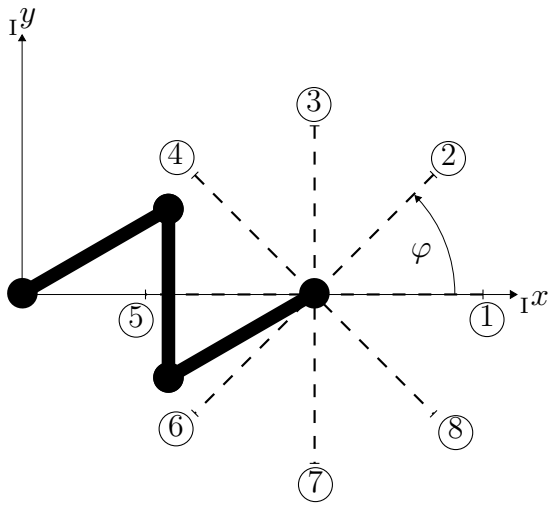

Figure A.1: Planar robot – Paths for tasks

Subtask 1: $\varphi = 0$

No convergence for $q_\mathrm{r} = q_3$.

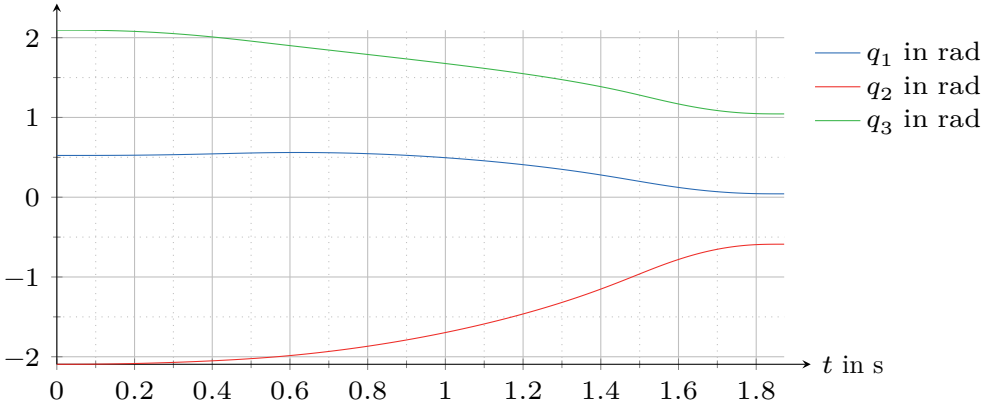

Figure A.2: Results for joint angles q_i for $q_\mathrm{r} = q_1$, $t_\mathrm{E} = 1.87$ s

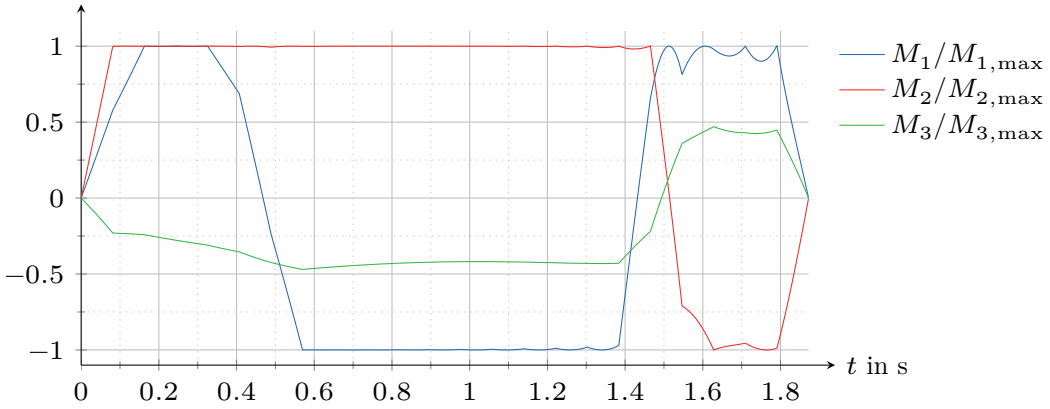

Figure A.3: Results for normalized joint torques for $q_\mathrm{r} = q_1$, $t_\mathrm{E} = 1.87$ s

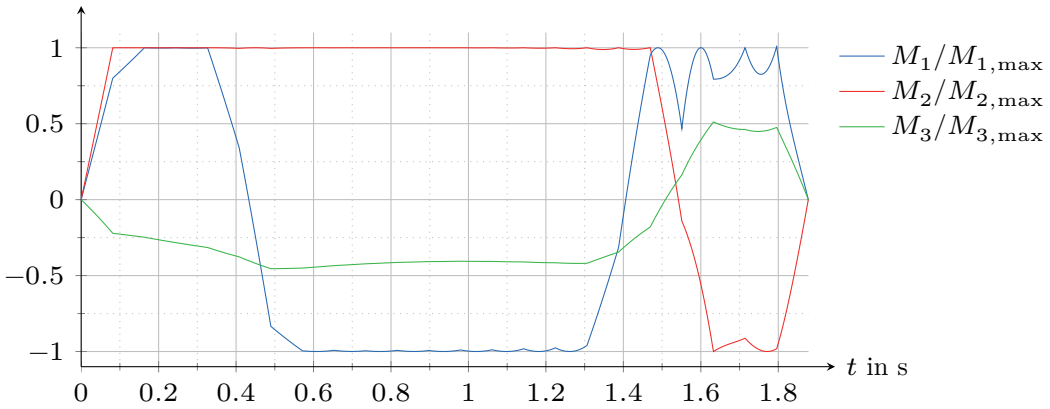

Figure A.4: Results for normalized joint torques for $q_\mathrm{r} = q_2$, $t_\mathrm{E} = 1.88$ s

Subtask 2: $\varphi = 45°$

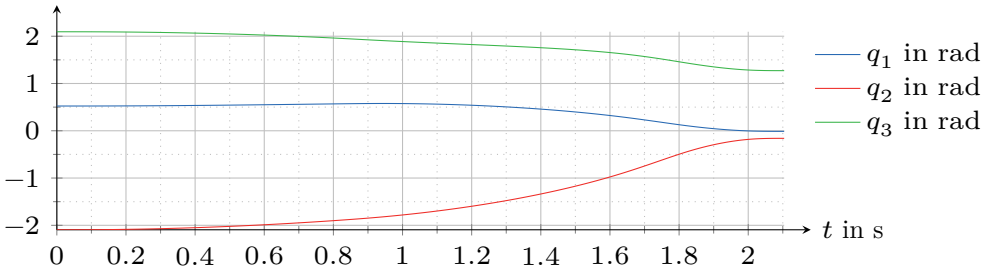

Figure A.5: Results for joint angles q_i for $q_\mathrm{r} = q_1$, $t_\mathrm{E} = 2.10$ s

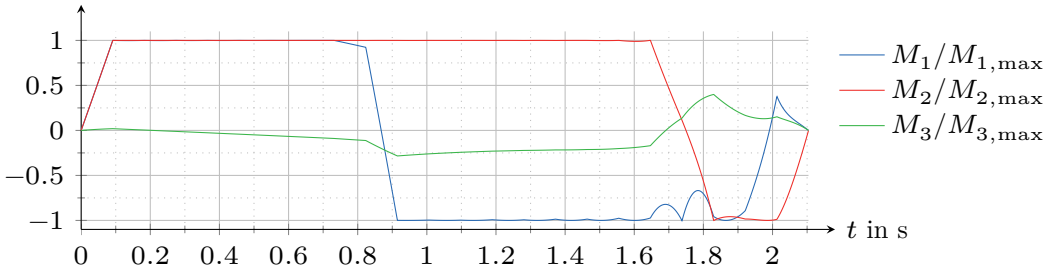

Figure A.6: Results for normalized joint torques for $q_\mathrm{r} = q_1$, $t_\mathrm{E} = 2.10$ s

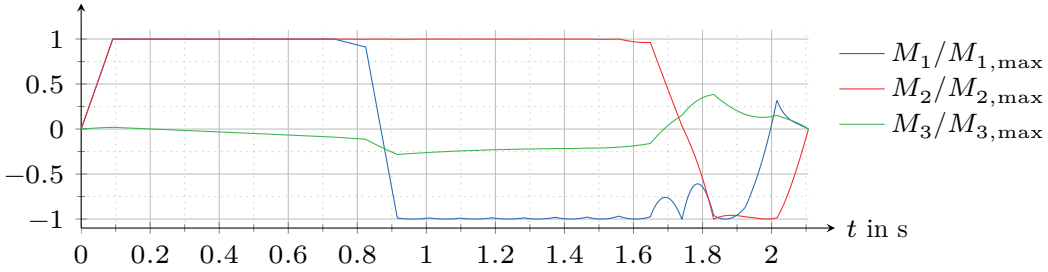

Figure A.7: Results for normalized joint torques for $q_\mathrm{r} = q_2$, $t_\mathrm{E} = 2.11$ s

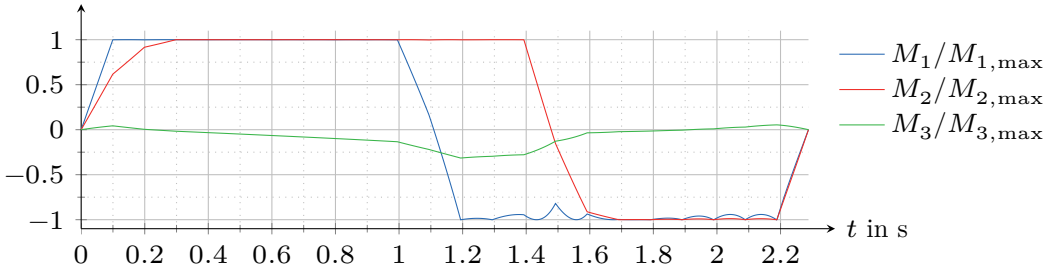

Figure A.8: Results for normalized joint torques for $q_\mathrm{r} = q_3$, $t_\mathrm{E} = 2.29$ s

Subtask 3: $\varphi = 90°$

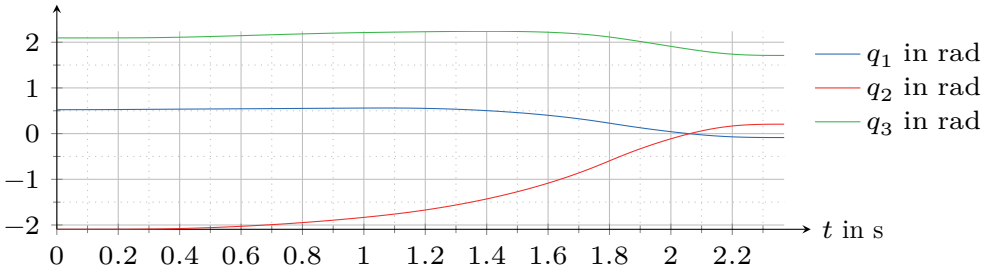

Figure A.9: Results for joint angles q_i for $q_\mathrm{r} = q_1$, $t_\mathrm{E} = 2.37$ s

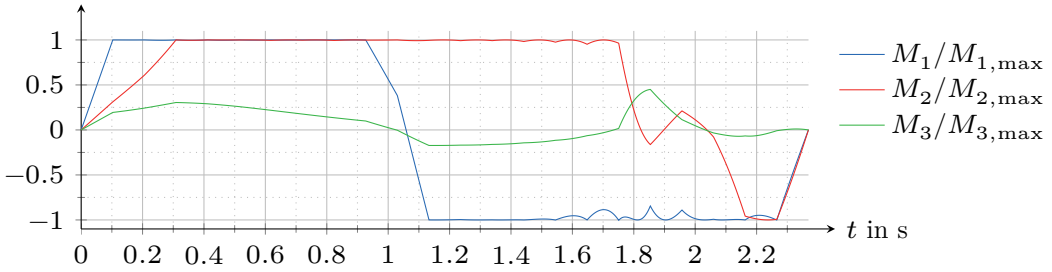

Figure A.10: Results for normalized joint torques for $q_\mathrm{r} = q_1$, $t_\mathrm{E} = 2.37$ s

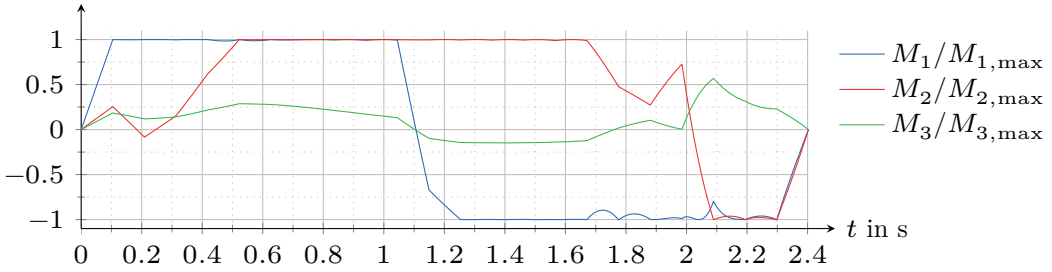

Figure A.11: Results for normalized joint torques for $q_\mathrm{r} = q_2$, $t_\mathrm{E} = 2.40$ s

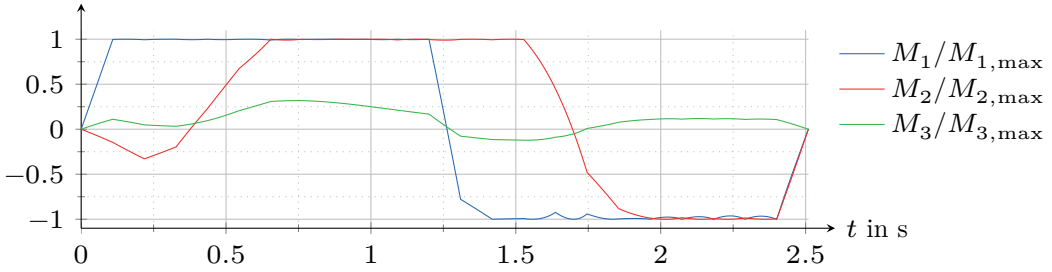

Figure A.12: Results for normalized joint torques for $q_\mathrm{r} = q_3$, $t_\mathrm{E} = 2.51$ s

Subtask 4: $\varphi = 135°$

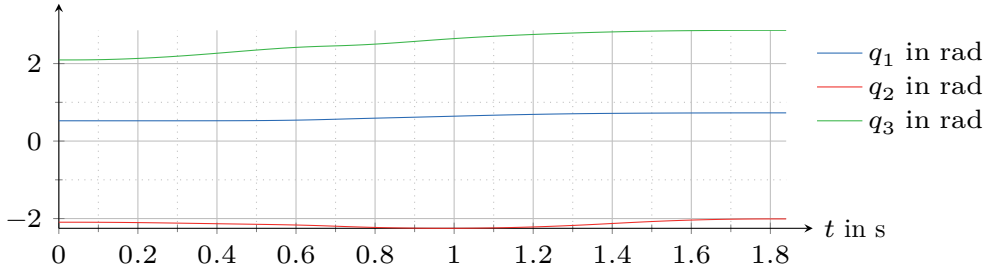

Figure A.13: Results for joint angles q_i for $q_\mathrm{r} = q_1$, $t_\mathrm{E} = 1.84$ s

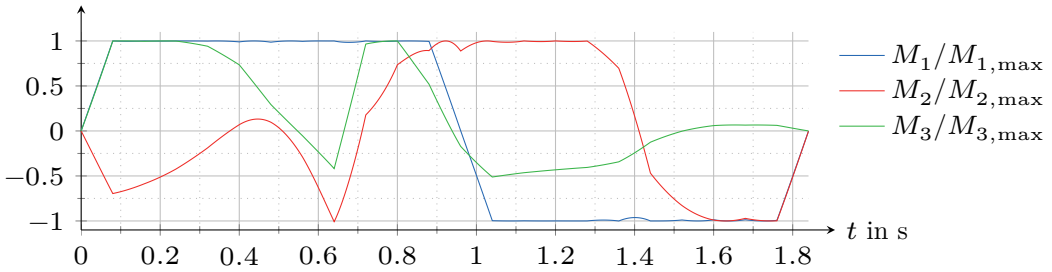

Figure A.14: Results for normalized joint torques for $q_\mathrm{r} = q_1$, $t_\mathrm{E} = 1.84$ s

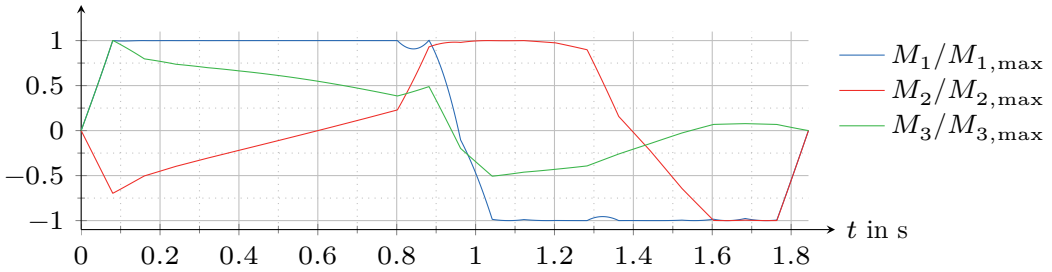

Figure A.15: Results for normalized joint torques for $q_\mathrm{r} = q_2$, $t_\mathrm{E} = 1.84$ s

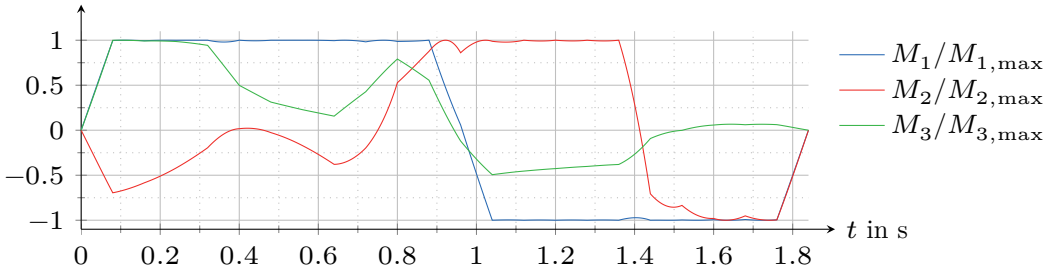

Figure A.16: Results for normalized joint torques for $q_\mathrm{r} = q_3$, $t_\mathrm{E} = 1.84$ s

Subtask 5: $\varphi = 180°$

No convergence for $q_\mathrm{r} = q_1$ and $q_\mathrm{r} = q_2$.

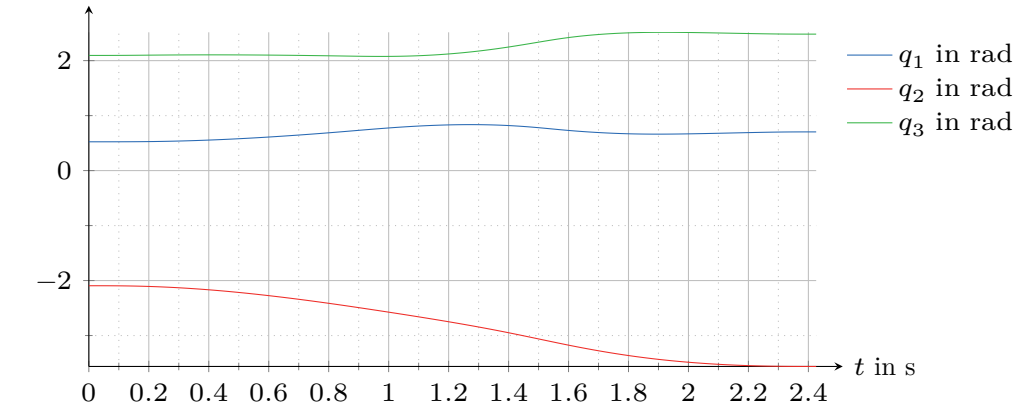

Figure A.17: Results for joint angles q_i for $q_\mathrm{r} = q_3$, $t_\mathrm{E} = 2.43$ s

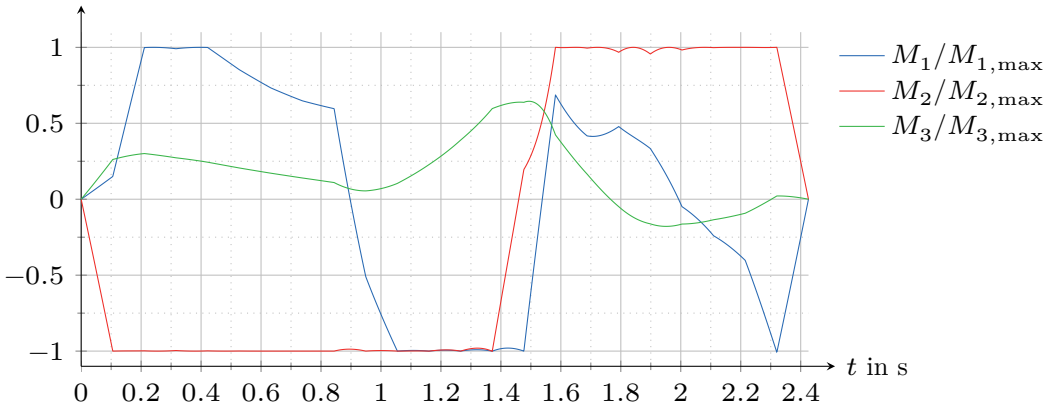

Figure A.18: Results for normalized joint torques for $q_\mathrm{r} = q_3$, $t_\mathrm{E} = 2.43$ s

Subtask 6: $\varphi = 225°$

No convergence for $q_\mathrm{r} = q_1$.

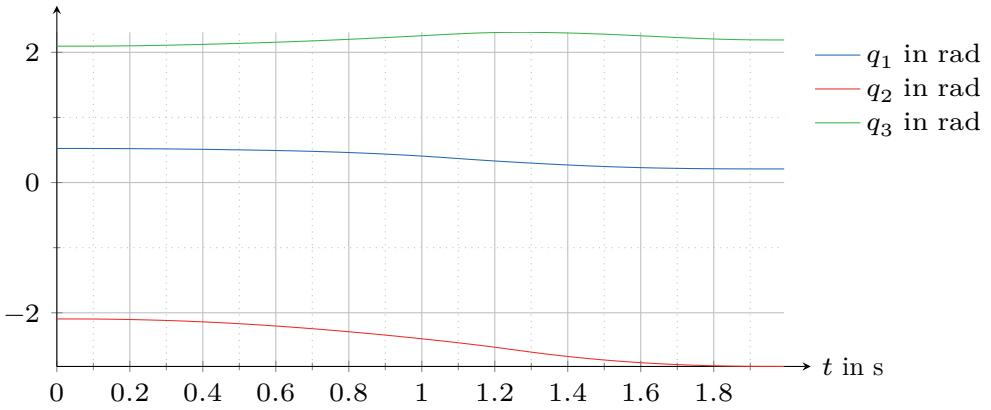

Figure A.19: Results for joint angles q_i for $q_\mathrm{r} = q_2$, $t_\mathrm{E} = 1.99$ s

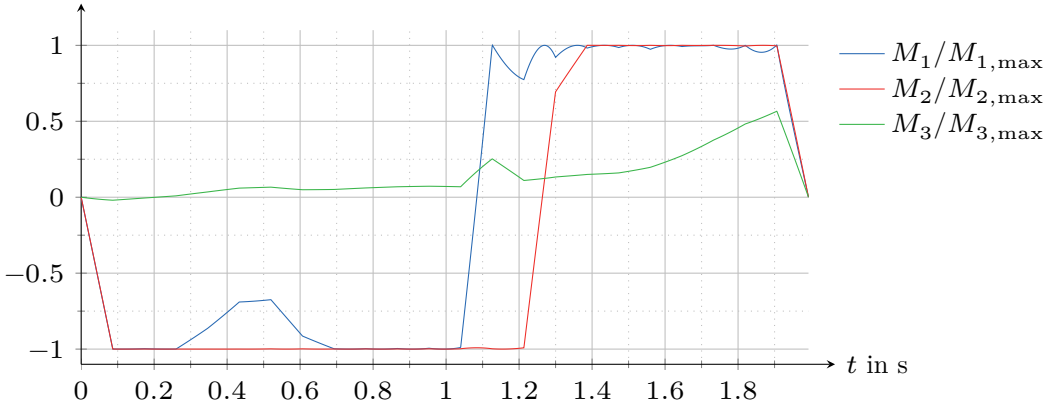

Figure A.20: Results for normalized joint torques for $q_\mathrm{r} = q_2$, $t_\mathrm{E} = 1.99$ s

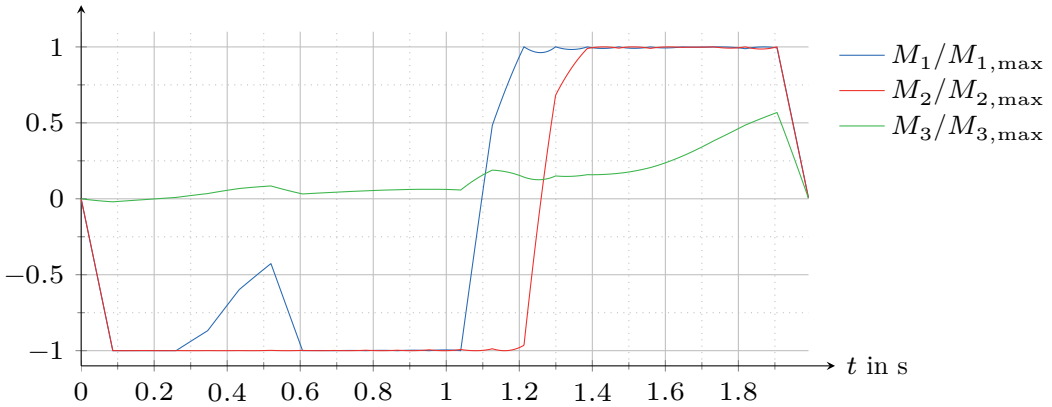

Figure A.21: Results for normalized joint torques for $q_\mathrm{r} = q_3$, $t_\mathrm{E} = 1.99$ s

Subtask 7: $\varphi = 270°$

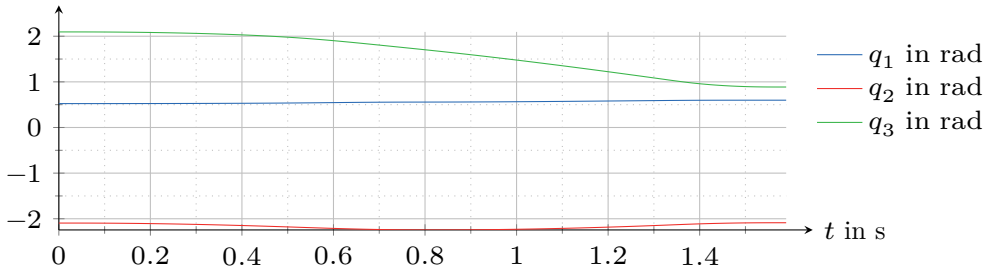

Figure A.22: Results for joint angles q_i for $q_\mathrm{r} = q_1$, $t_\mathrm{E} = 1.59$ s

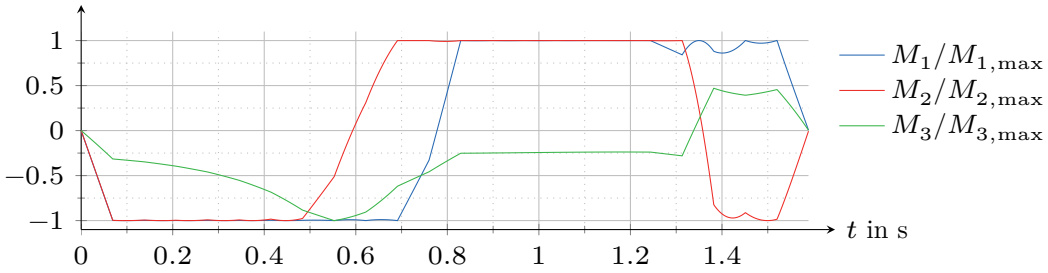

Figure A.23: Results for normalized joint torques for $q_\mathrm{r} = q_1$, $t_\mathrm{E} = 1.59$ s

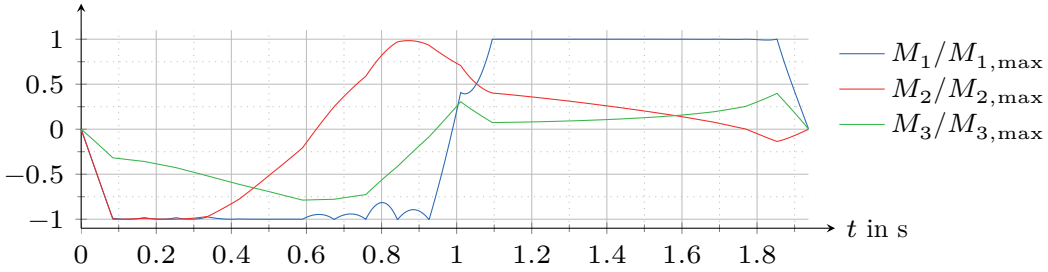

Figure A.24: Results for normalized joint torques for $q_\mathrm{r} = q_2$, $t_\mathrm{E} = 1.94$ s

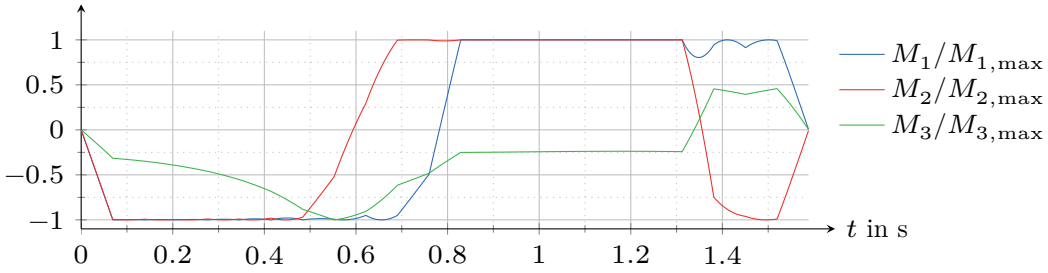

Figure A.25: Results for normalized joint torques for $q_\mathrm{r} = q_3$, $t_\mathrm{E} = 1.59$ s

Subtask 8: $\varphi = 315°$

No convergence for $q_\mathrm{r} = q_2$.

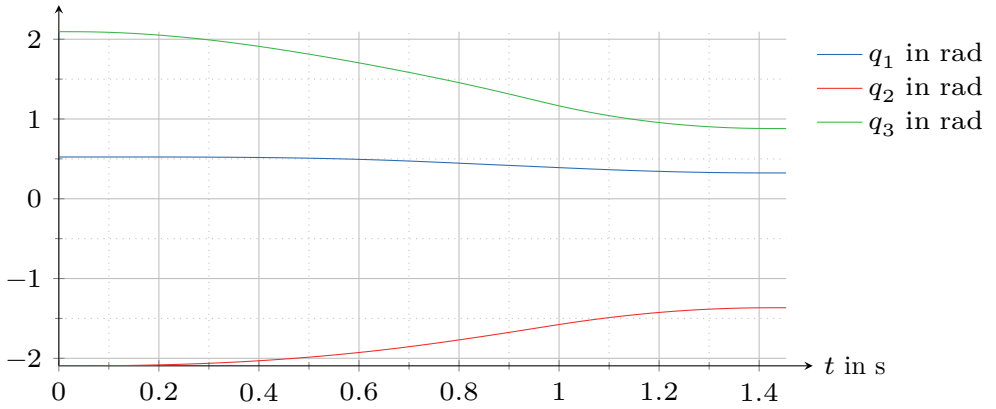

Figure A.26: Results for joint angles q_i for $q_\mathrm{r} = q_1$, $t_\mathrm{E} = 1.45$ s

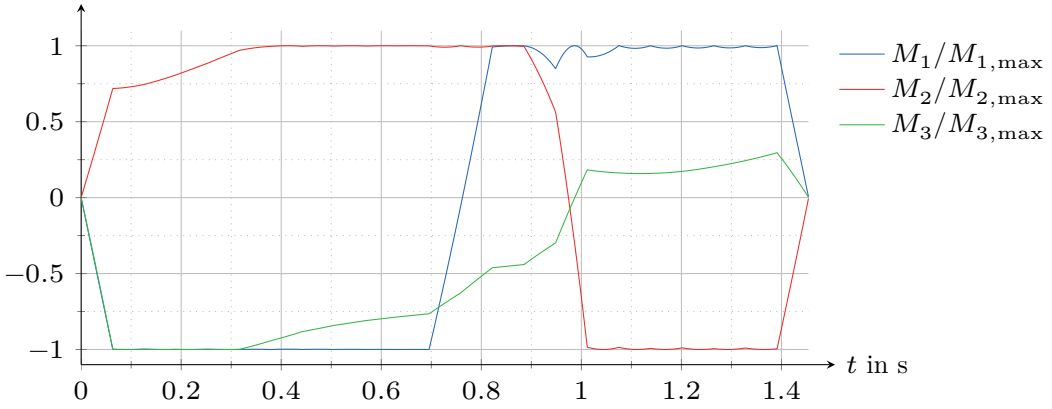

Figure A.27: Results for normalized joint torques for $q_\mathrm{r} = q_1$, $t_\mathrm{E} = 1.45$ s

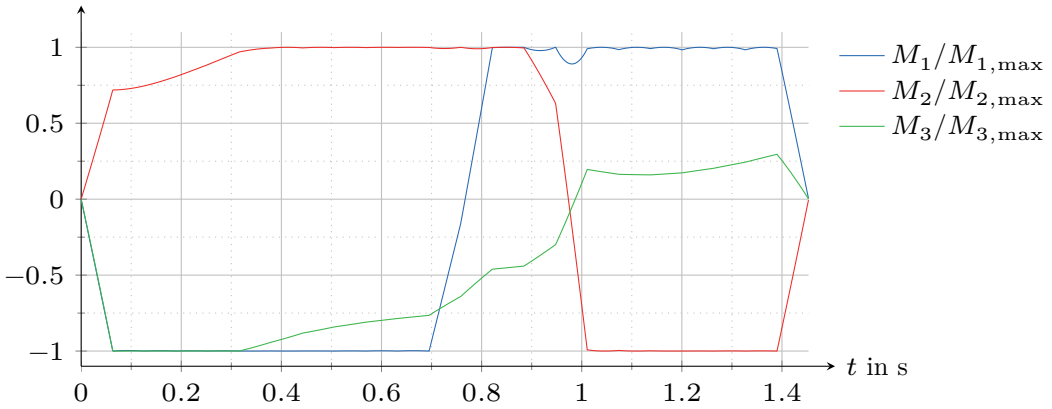

Figure A.28: Results for normalized joint torques for $q_\mathrm{r} = q_3$, $t_\mathrm{E} = 1.45$ s

Appendix B

Results for the spatial example

This section includes detailed results of the example from Section 6.2. The position of the testing cube from Figure B.1 is detailed in Table B.1 on the next page.

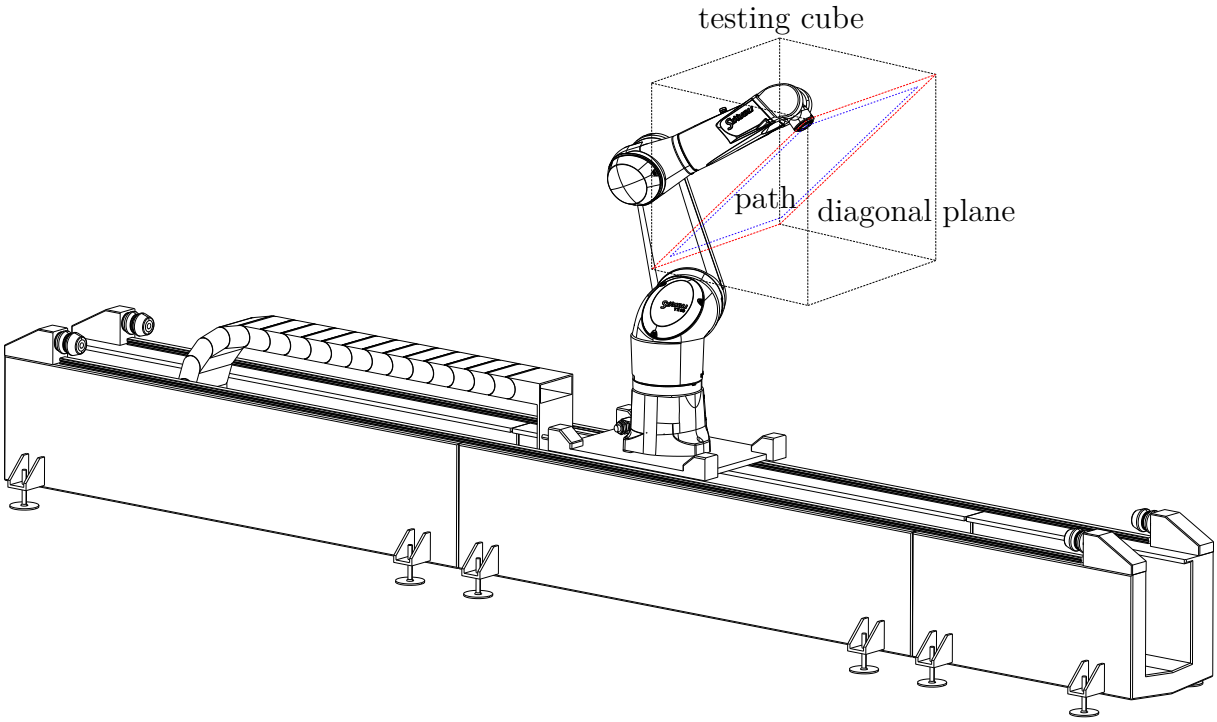

Figure B.1: Industrial robot with rectangular path in testing cube

For quick reference, the task specific choices for the respective inverse kinematics configuration from Table B.2 on the next page.

Table B.1: Initial positions for subtasks

Subtask	${}_{\mathrm{I}}x$ in m	${}_{\mathrm{I}}y$ in m	${}_{\mathrm{I}}z$ in m
1	2.5	0	0.7
2	2.5	0.63	0.7
3	2.85	0.63	0.7
4	3.15	0.63	0.8
5	3.5	0.22	0.87

Table B.2: Inverse kinematics solution for subtasks

Subtask	$\pm_1$	$\pm_2$	$\pm_3$
1	+	+	+
2	−	−	+
3	+	+	+
4	−	−	+
5	−	−	+

The physical limits imposed on the optimization problem can be found in Table B.3 for quick reference.

Table B.3: Physical limits of industrial robot

Joint i	Gear ratio	$M_{i,\max}(\pm)$	$\ddot{q}_{i,\max}$ $(\pm)$	$\dot{q}_{i,\max}(\pm)$	$q_{i,\min}$	$q_{i,\max}$
1	114.2727	69 Nm	15 m/s^2	4 m/s	0 m	2.55 m
2	32	42 Nm	770°/s^2	400°/s	−180°	180°
3	32	42 Nm	482°/s^2	400°/s	−130°	147.5°
4	32	17.5 Nm	1084°/s^2	400°/s	−145°	145°
5	32	4.5 Nm	3082°/s^2	500°/s	−270°	270°
6	45	3.4 Nm	2042°/s^2	450°/s	−115°	140°
7	30	2.2 Nm	6000°/s^2	720°/s	−270°	270°

The following plots of the joint velocities $\dot{q}_i$, the joint accelerations $\ddot{q}_i$ and the joint torques M_i are normalized with respect to their respective limits. The joint positions q_i are normalized with respect to their feasible interval by means of the expression

$$q_{i,\mathrm{norm}} = \frac{q_i - q_{i,\min}}{q_{i,\max} - q_{i,\min}}.$$

Subtask 1

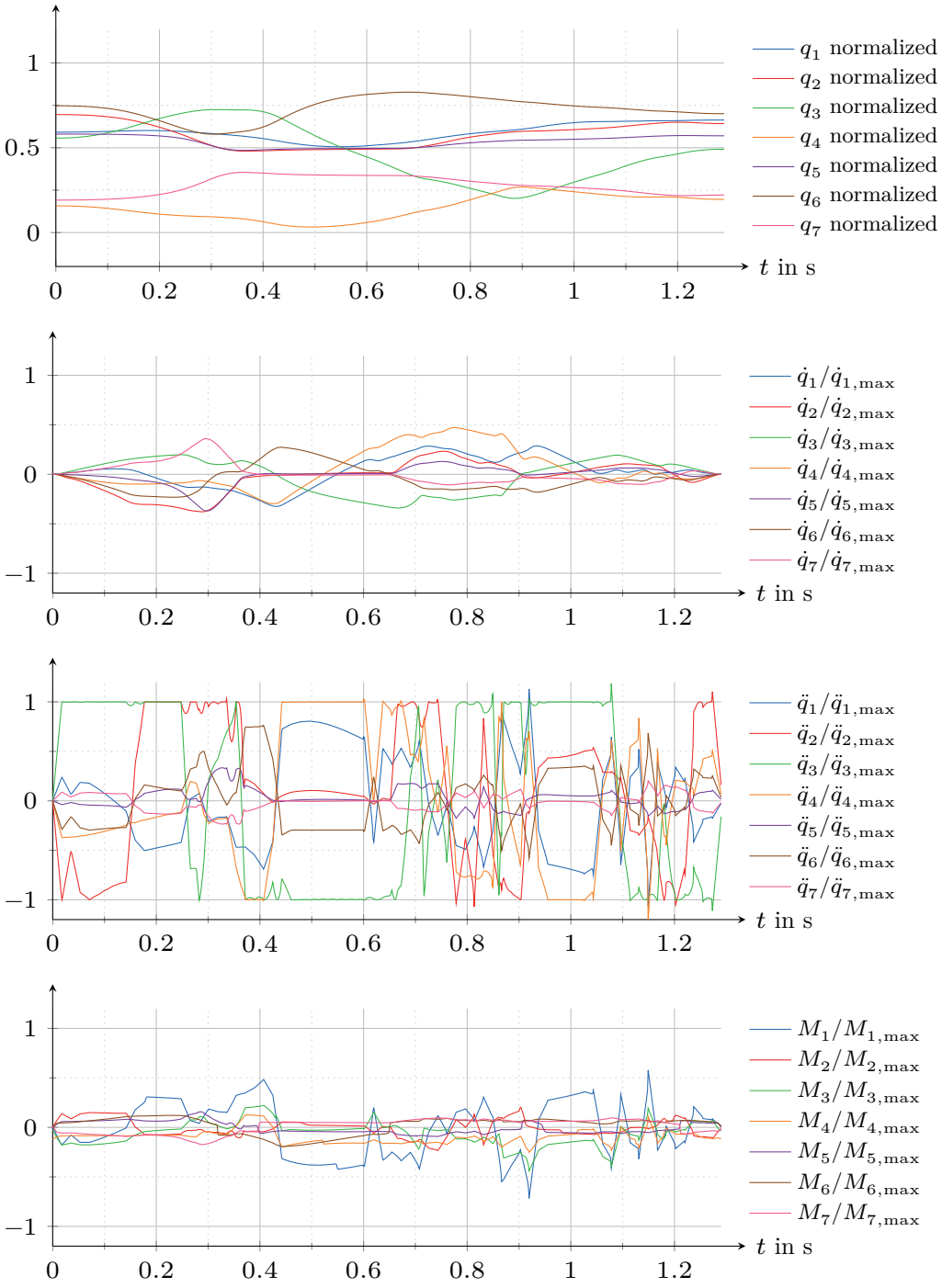

Figure B.2: Spatial robot — Separation approach, results for subtask 1, $t_E = 1.29$ s

Subtask 2

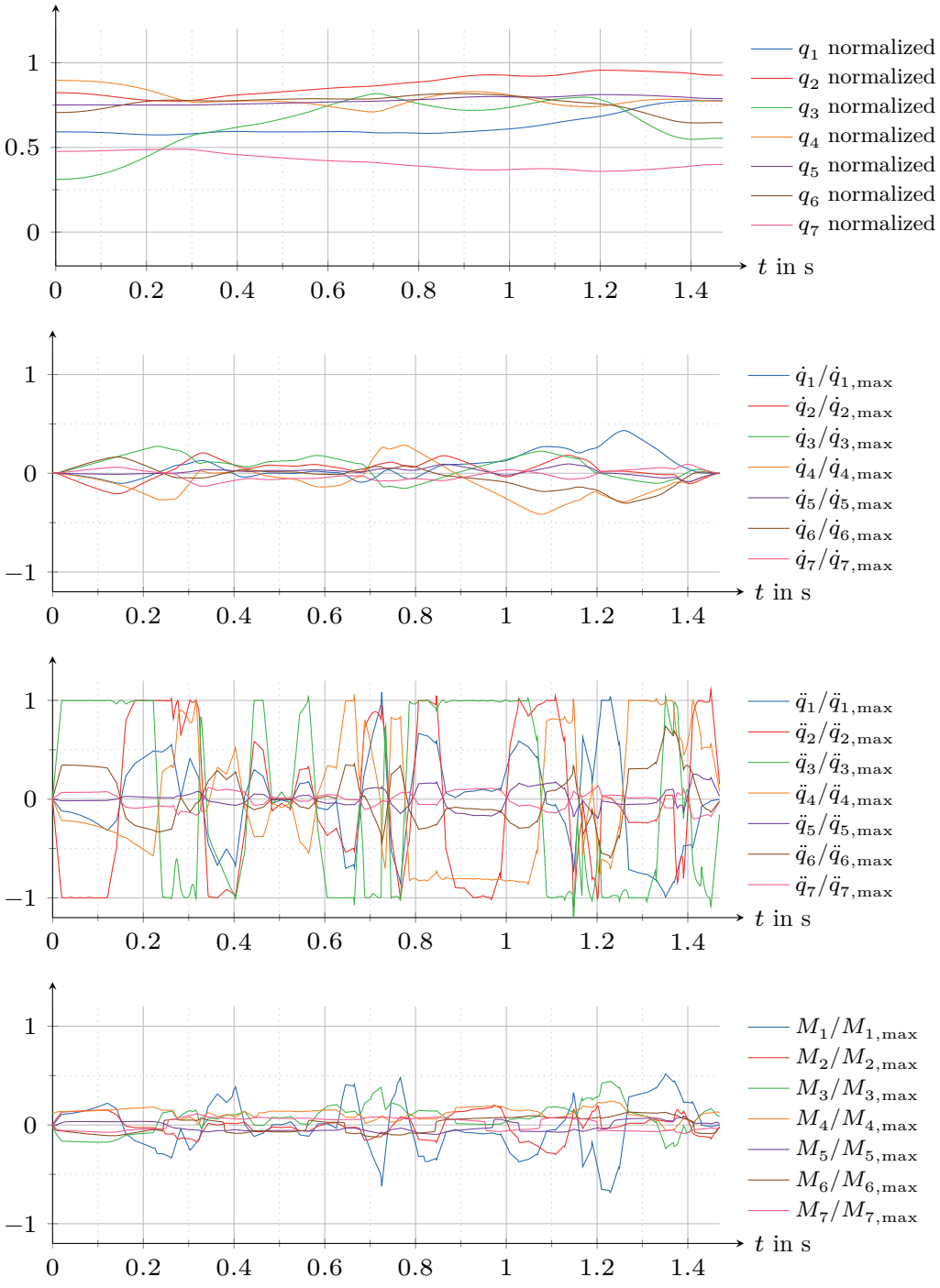

Figure B.3: Spatial robot — Separation approach, results for subtask 2, $t_E = 1.47$ s

Subtask 3

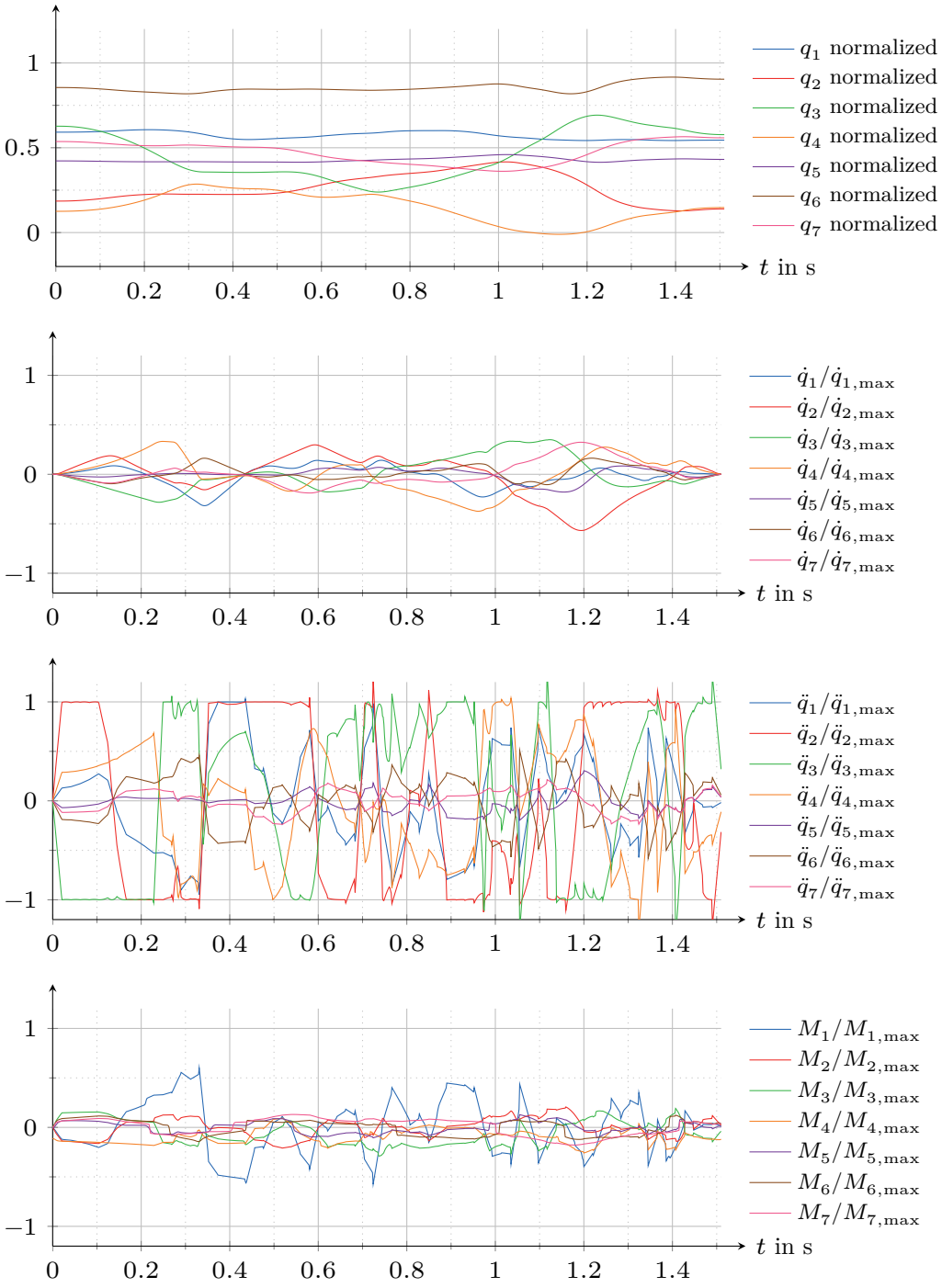

Figure B.4: Spatial robot — Separation approach, results for subtask 3, $t_E = 1.52$ s

Subtask 4

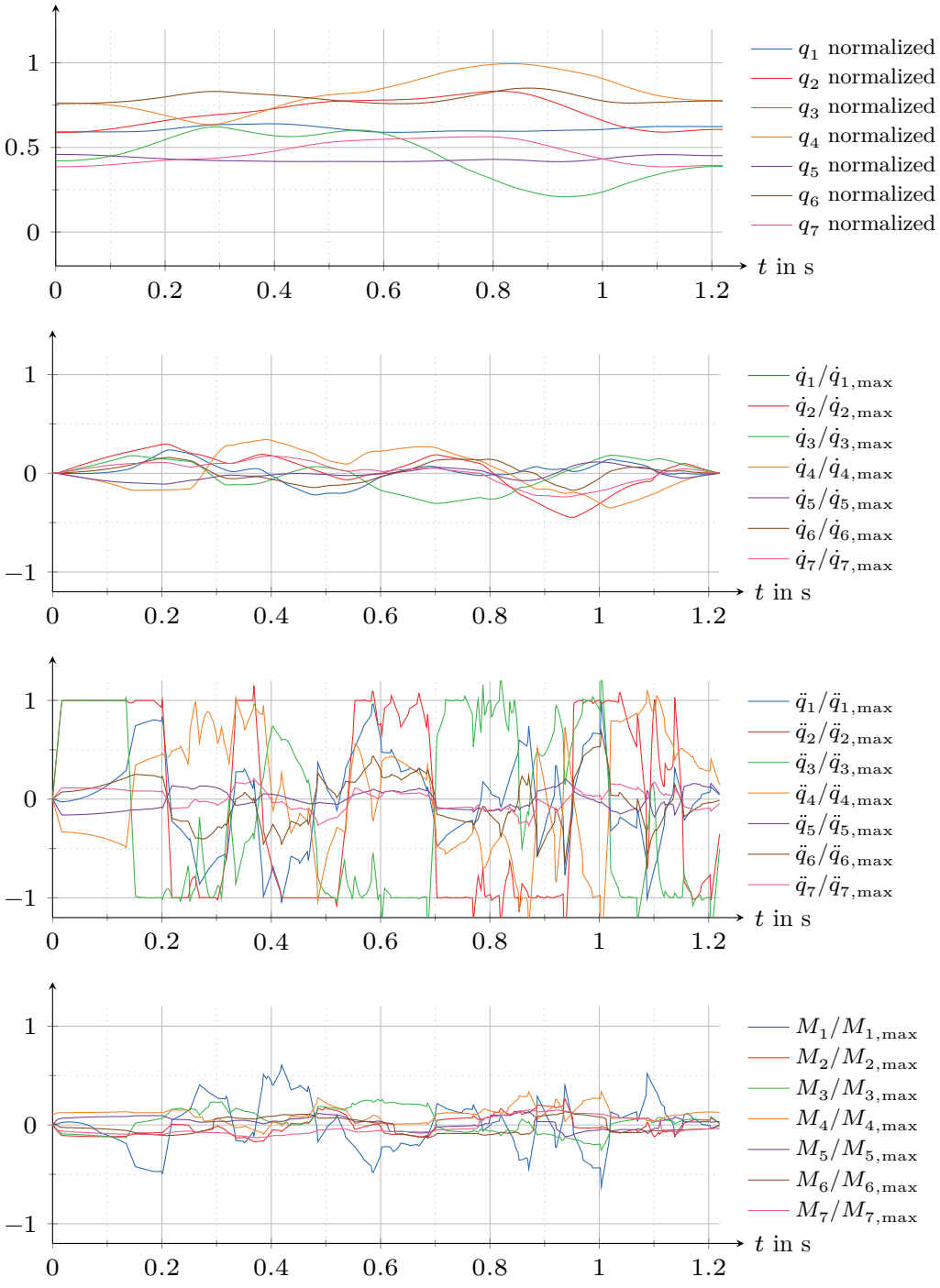

Figure B.5: Spatial robot — Separation approach, results for subtask 4, $t_E = 1.23$ s

Subtask 5

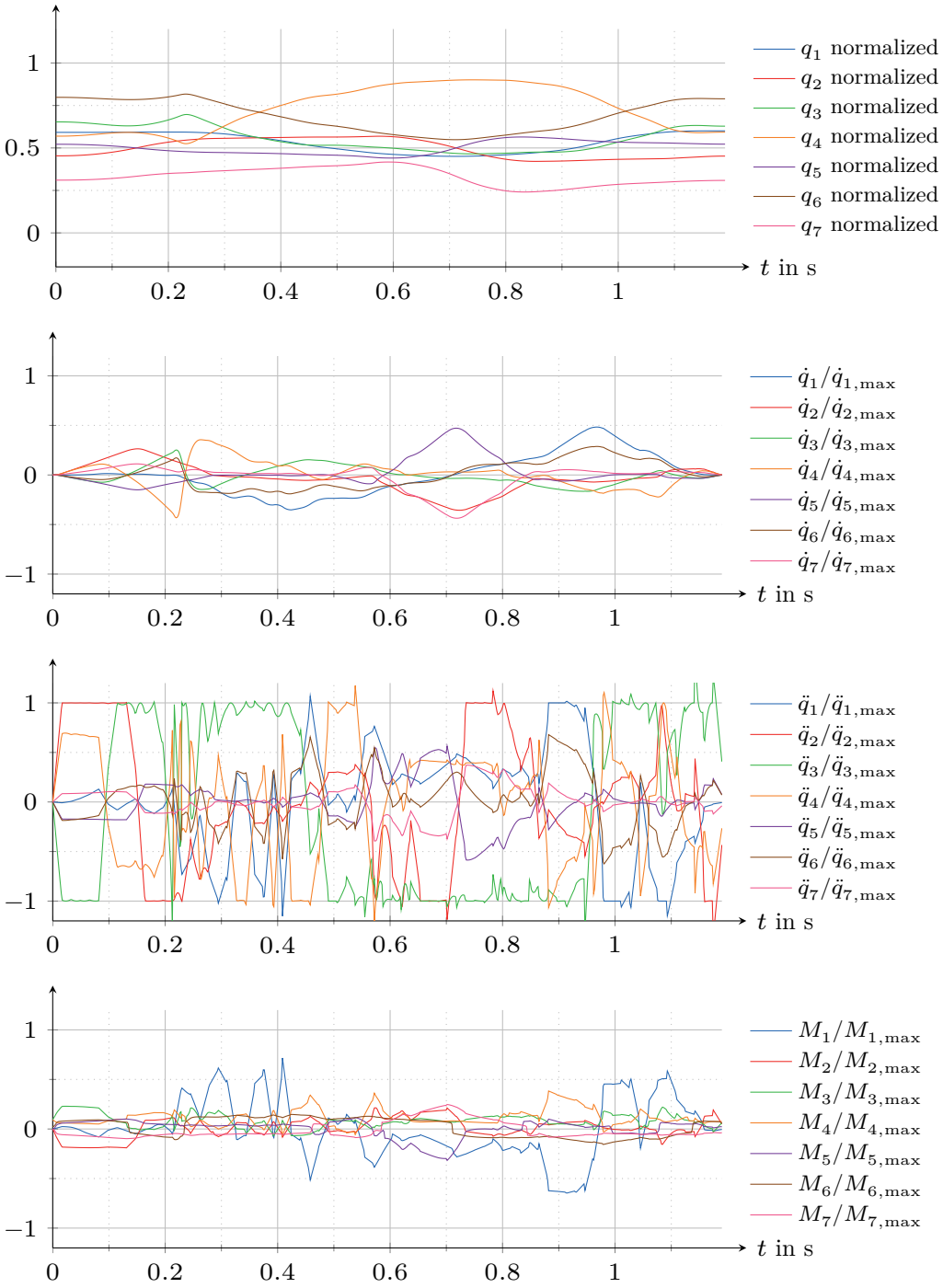

Figure B.6: Spatial robot — Separation approach, results for subtask 5, $t_\mathrm{E} = 1.20$ s

http://www.springer.com/978-3-658-12700-8

Time-Optimal Trajectory Planning for Redundant Robots
Joint Space Decomposition for Redundancy Resolution
in Non-Linear Optimization
Reiter, A.
2016, XV, 90 p. 35 illus., Softcover
ISBN: 978-3-658-12700-8